

Martin G. Mack, MD
Jörn O. Balzer, MD
Ralf Straub, MD
Katrin Eichler, MD
Thomas J. Vogl, MD

Index terms:

Head and neck neoplasms, 26.373, 27.373
Iron, 276.12143
Lymphatic system, MR, 276.121411, 276.121412, 276.12143
Lymphatic system, neoplasms, 276.375
Magnetic resonance (MR), contrast media, 276.12143

Published online before print
10.1148/radiol.2221010225
Radiology 2002; 222:239–244

Abbreviations:

GRE = gradient echo
ROI = region of interest
SE = spin echo
SI = signal intensity
SPIO = superparamagnetic iron oxide

¹ From the Department of Diagnostic and Interventional Radiology, University of Frankfurt/Main, Theodor-Stern-Kai 7, 60590 Frankfurt am Main, Germany. Received January 4, 2001; revision requested February 28; revision received April 2; accepted May 21. Address correspondence to M.G.M. (e-mail: m.mack@em.uni-frankfurt.de).

© RSNA, 2001

Author contributions:

Guarantors of integrity of entire study, M.G.M., T.J.V.; study concepts and design, M.G.M., T.J.V.; literature research, M.G.M., J.O.B.; clinical studies, all authors; data acquisition, M.G.M., K.E.; data analysis/interpretation, M.G.M., J.O.B., T.J.V.; statistical analysis, M.G.M.; manuscript preparation, M.G.M., J.O.B.; manuscript definition of intellectual content and editing, M.G.M., T.J.V.; manuscript revision/review, M.G.M., R.S., K.E.; manuscript final version approval, all authors.

Superparamagnetic Iron Oxide–enhanced MR Imaging of Head and Neck Lymph Nodes¹

PURPOSE: To compare findings on superparamagnetic iron oxide (SPIO)–enhanced magnetic resonance (MR) images of the head and neck with those from resected lymph node specimens and to determine the effect of such imaging on surgical planning in patients with histopathologically proved squamous cell carcinoma of the head and neck.

MATERIALS AND METHODS: Thirty patients underwent MR imaging with non-enhanced and SPIO-enhanced (2.6 mg Fe/kg intravenously) T1-weighted (500/15 [repetition time msec/echo time msec]) and T2-weighted (1,900/80) spin-echo and T2-weighted gradient-echo (GRE) (500/15, 15° flip angle) sequences. Signal intensity decrease was measured, and visual analysis was performed. Surgical plans were modified, if necessary, according to MR findings. Histopathologic and MR findings were compared.

RESULTS: Histopathologic evaluation of 1,029 lymph nodes revealed 69 were metastatic. MR imaging enabled detection of 59 metastases. Regarding lymph node levels, MR diagnosis was correct in 26 of 27 patients who underwent surgery: Only one metastasis was localized in level II with MR imaging, whereas histopathologic evaluation placed it at level III. Extent of surgery was changed in seven patients. SPIO-enhanced T2-weighted GRE was the best sequence for differentiating between benign and malignant lymph nodes.

CONCLUSION: SPIO-enhanced MR imaging has an important effect on planning the extent of surgery. On a patient basis, SPIO-enhanced MR images compared well with resected specimens.

In the head and neck region, cross-sectional imaging techniques—magnetic resonance (MR) imaging, computed tomography (CT), and ultrasonography (US)—allow visualization of lymph nodes that may not be palpable at physical examination (1). The diagnosis of lymph node metastases is based mainly on measurement of nodal dimensions, such as maximum transverse diameter (2–8) or ratios of maximum longitudinal to maximum transverse diameter (9). The enhancement pattern, shape, and grouping of lymph nodes are further criteria with less importance. All of these criteria remain controversial, and recommendations for differentiating between benign and malignant lymph nodes with imaging studies vary widely (2–8,10).

The currently applied morphologic criteria allow clear differentiation only between benign lymph nodes and large metastatic lymph nodes with central necrosis or extracapsular spread. Lymph node metastases in the head and neck region, however, often will be less than 10 mm, occasionally even less than 5 mm, in diameter (11).

Intravenously injected small iron oxide particles pass through the vascular endothelium into the interstitium and are eventually taken up by normally functioning lymph nodes and inflamed lymph nodes, to be phagocytosed by components of the reticuloendothelial system, such as macrophages or histiocytes. These normal lymph nodes show a signal intensity (SI) decrease on T2*- and T2-weighted MR images because of the effects of magnetic susceptibility and T2 shortening on the iron deposits. Metastatic lymph nodes,

however, have lost their mechanism for phagocytosis and, therefore, do not show the reduced SI, which potentially allows them to be differentiated from benign lymph nodes.

The purposes of our study were to compare findings on superparamagnetic iron oxide (SPIO)-enhanced MR images of the head and neck with those of resected lymph node specimens and to determine the effect of such imaging findings on surgical planning in patients with histopathologically proved squamous cell carcinoma of the head and neck.

MATERIALS AND METHODS

Contrast Agent

The iron contrast agent Sinerem (Guerbet, Paris, France) was provided as a lyophilized powder consisting of ultrasmall SPIO particles covered with low-molecular-weight dextran, with a total particle diameter in solution between 170 and 210 Å (17–21 nm).

The contrast agent (2.6 mg of iron per kilogram of body weight) was administered intravenously in a single dose by drip infusion through an infusion filter (0.22- μ m pore size) at a rate of 4 mL/min. It was diluted in 100 mL of saline.

This study was part of a multicenter phase III clinical trial and was approved by the ethics committee; informed consent was obtained from the patients.

Inclusion and Exclusion Criteria

The inclusion criteria were as follows: (a) patients aged 18 years or older of either sex (female patients who used effective contraception [contraceptive pill or intrauterine device] or who were surgically sterilized or postmenopausal [amenorrhea for at least 12 months]); (b) patients with newly diagnosed, untreated head and neck squamous cell carcinoma, which was confirmed at histopathologic examination, regardless of TNM stage; or (c) patients scheduled to undergo surgery with lymphadenectomy within 10 days of MR imaging with the SPIO contrast agent.

The exclusion criteria were as follows: (a) patients with a contraindication to MR imaging; (b) patients with a known allergy to dextran or drugs containing iron salts; (c) patients in a precarious hemodynamic state, with risk of decompensation after administration of the SPIO contrast agent; (d) patients who received gadolinium complexes within 2 days or iron oxide nanoparticles within 7 days before MR imaging (nonenhanced

MR imaging and MR imaging with the SPIO contrast agent); (e) patients who underwent chemotherapy before surgery; (f) patients who underwent radiation therapy to the area to be investigated; (g) patients in whom the tumor had already been resected at lymphadenectomy; (h) female patients who were breast-feeding; (i) patients participating in another clinical trial, including that of an investigational drug; (j) patients under guardianship; or (k) patients whose degree of cooperation was incompatible with carrying out the study.

Patients

Thirty consecutive patients (26 men, four women; mean age, 55.7 years; age range, 41–71 years) who met our inclusion criteria were examined. Their types of tumors were as follows: laryngeal cancer ($n = 9$), oropharyngeal cancer ($n = 11$), hypopharyngeal cancer ($n = 5$), and cancer of the floor of the mouth ($n = 5$). According to the results of clinical examination and US evaluation, 29 patients had metastatic involvement of the lymph nodes of the neck.

Imaging Technique

All MR examinations were performed with a 1.5-T magnet (Magnetom SP4000; Siemens, Erlangen, Germany) by using conventional T1-weighted (500/15 [repetition time msec/echo time msec]) and T2-weighted (1,900/80) spin-echo (SE) sequences and a T2-weighted gradient-echo (GRE) (500/15, 15° flip angle) sequence. The T1-weighted SE and the GRE images were obtained in transverse and coronal orientations. Section thickness was 5 mm with a 1-mm intersection gap for all transverse sequences. Coronal imaging was performed without an intersection gap. All lymph nodes of level I to VII were imaged at least in the transverse orientation. All sequences were performed before and after administration of the SPIO contrast agent. SPIO-enhanced MR imaging was performed within 24–36 hours after the end of the contrast material injection due to a maximum iron peak in lymph nodes, spleen, and liver between 1 and 3 days after injection. The mean duration between nonenhanced and SPIO-enhanced MR imaging was 30.3 hours.

Evaluation

Metastatic lymph node involvement was evaluated by examining the neck of each patient and by examining individ-

ual nodes. The nodes were grouped according to guidelines of the American Joint Committee on Cancer and a simplified level classification (7,12). Lymph node SI was evaluated on the nonenhanced and SPIO-enhanced MR images (all three sequences) by using a region-of-interest (ROI) evaluation in relation to the background noise. The size of the ROI for the background noise was fixed to 1 cm in diameter. The mean value of the measurements obtained in each corner of the image was used for further calculations. The size of the ROI was adjusted to the size of the lymph node in a range between 5 mm and 3 cm. In each patient, we performed SI measurements of all malignant lymph nodes and of 20 benign lymph nodes for comparison. The SI ratio for each node was determined as follows: SI ratio = (SI_{node}/SI_{background} on SPIO-enhanced images)/(SI_{node}/SI_{background} on nonenhanced images). Because this contrast agent has predominantly T2* shortening effects, low SI ratios represent decreased SI of nodes, which is expected with normal or benign nodes, whereas high SI ratios represent metastatic nodes. SI ratios were finally presented as a percentage decrease in SI (eg, SI ratio = 0.3 = 70% decrease in SI).

For statistical analysis, the nested analysis of variance was used for comparing the SI ratios. Sensitivity, specificity, and positive and negative predictive values were calculated on a node-by-node basis, assuming the independence of the nodes.

The size of the lymph nodes was further evaluated. The short and the long axes were measured, where the longitudinal dimension was measured perpendicular to the short axis.

Visual analysis was based on the following criteria: Nonenhanced and SPIO-enhanced images were compared. Lymph nodes with a homogeneous SI decrease on SPIO-enhanced images compared with SI on nonenhanced images were considered normal lymph nodes. Those with no SI decrease on SPIO-enhanced images compared with SI on nonenhanced images were considered metastatic lymph nodes. Those with a partial SI decrease on SPIO-enhanced images compared with SI on nonenhanced images were considered lymph nodes with partial metastatic infiltration. The prospective criterion for judging a lymph node to be positive or negative was based on SI characteristics alone, and it was a qualitative and quantitative judgment.

The image evaluation was performed by two experienced head and neck radi-

ologists (M.G.M., T.J.V.) by consensus. Nonenhanced and SPIO-enhanced images were available to both radiologists at the same time.

Discomfort and adverse reactions were recorded during at least 24 hours after the start of injection. A written report containing the evaluation of the nonenhanced and SPIO-enhanced images was made, and images were discussed with the surgeons. The surgical plan was based on clinical, endoscopic, and US evaluation, with use of size and shape information obtained before MR imaging, and was reviewed and modified, if necessary, on the basis of the MR imaging results.

The primary tumor was removed, and a radical or limited neck dissection was performed within 10 days of SPIO-enhanced MR imaging. On the basis of the MR imaging findings, three patients were no longer candidates for surgery because of extensive tumor infiltration in combination with unresectable lymph node metastases. The mean duration between the end of injection and surgery was 3.92 days (range, 1–10 days). The influence of the results of SPIO-enhanced MR imaging on surgical strategy was documented.

Resected specimens were analyzed histopathologically by the pathologist, and the results were compared with those of nonenhanced and SPIO-enhanced MR imaging. Specific lymph nodes were compared together by the surgeon, the pathologist, and the radiologist, by using the patient's MR images, with needle marking of the specimen. However, comparison for all lymph nodes was not possible, especially in patients who received only a limited neck dissection. With histopathologic examination as the reference standard, sensitivity, specificity, and positive and negative predictive values for nodes depicted on SPIO-enhanced MR images were calculated.

RESULTS

Twenty-nine of the 30 patients tolerated the injection of contrast agent without any discomfort or adverse reactions. In one patient, the injection was interrupted at 5 minutes because of nausea and vertigo. However, the patient recovered within 20 minutes, and injection of the contrast agent was continued at a slower rate. There were no further complications.

The three patients who were no longer candidates for surgery because of extensive tumor infiltration in combination

with unresectable lymph node metastases underwent primary radiation therapy. The extensive tumor infiltration in these patients was demonstrated on the nonenhanced MR images.

Therefore, histopathologic evaluation was available for 27 patients who underwent surgery, which yielded a total of 1,029 lymph nodes in 27 patients. Sixty-nine of these lymph nodes showed metastatic involvement, and 960 were benign. All 1,029 lymph nodes could be identified at least on SPIO-enhanced T2-weighted GRE images. MR imaging enabled correct diagnosis of 59 of the 69 lymph node metastases.

Image Analysis

Although visual analysis demonstrated even benign lymph nodes smaller than 4 mm in diameter on MR images, SI measurements were not performed in lymph nodes smaller than 4 mm and were not performed in the lymph nodes of the three patients who did not undergo neck dissection because of extensive disease. Therefore, SI values were obtained for the 59 histopathologically proved lymph node metastases that were detected with MR imaging and for 540 benign lymph nodes (20 benign lymph nodes per patient for 27 patients).

In all patients, an obvious SI decrease was seen in benign lymph nodes on T2-weighted GRE images (mean, -71.6% ; range, -51.0% to -87.9%). A moderate SI decrease was observed in benign lymph nodes on the T2-weighted SE images (mean, -40.4% ; range, -29.6% to -48.9%). Lymph node metastases showed almost no SI change after administration of SPIO contrast material (mean, $+13.8\%$; range, -28.5% to $+6.4\%$). There was no relevant SI decrease in benign and malignant lymph nodes on T1-weighted SE images (mean, -2.3% ; range, -10.2% to $+8.7\%$) (Figs 1, 2). Quantitative measurements on T2-weighted GRE and SE images demonstrated no overlap between benign and malignant lymph nodes. The SI ratio for benign lymph nodes was significantly lower than that for metastatic lymph nodes ($P < .001$).

Statistical evaluation on a node-by-node basis documented a sensitivity of 86% (59 of 69), a specificity of 100% (960 of 960), a positive predictive value of 100% (59 of 59), and a negative predictive value of 99% (960 of 970). The evaluation on a patient-by-patient basis revealed a congruent diagnosis regarding node staging in all patients.

Visual analysis of the lymph nodes on

MR images was concordant with the results of quantitative analysis of SI in all 59 lymph node metastases, as well as in the 540 benign lymph nodes in which SI measurements were performed.

On the basis of the MR measurements, the minimum transverse diameter of lymph node metastases ranged between 8 and 40 mm (mean, 18 mm). The maximum diameter of lymph node metastases was between 8 and 60 mm (mean, 24 mm). The minimum diameter of the benign lymph nodes was 2 mm, and the maximum diameter was 19 mm (mean, 5 mm).

Histopathologic Correlation

On a node-by-node basis, the reduced number ($n = 10$) of lymph node metastases detected with MR imaging was due to false interpretation of the number of metastases ($n = 7$) that were contained in clusters on the MR images. The remaining three metastases were staged as benign lymph nodes on the MR images. These three lymph nodes were 6, 7, and 12 mm, respectively, in maximum diameter. Histopathologic evaluation demonstrated metastatic infiltration of less than 30% of the volume of these three lymph nodes. Most likely based on the limited resolution of the sequences used during this study, even retrospectively we were not able to delineate the partial infiltration clearly in these three nodes. The SI decrease in these three lymph nodes was somewhat less homogeneous; however, no areas without SI change could be detected. Finally, 26 of 27 patients had at least one lymph node metastasis.

In the level-by-level correlation, MR imaging and histopathologic examination resulted in congruent diagnosis in 26 of 27 patients. In one patient with a solitary lymph node metastasis, the metastasis was detected at both histopathologic evaluation and MR imaging. However, MR imaging localized this metastasis in level II, while at histopathologic evaluation it was classified as level III. Because no further lymph node metastases could be found in this patient, it was probable that the same metastasis was detected with both methods.

In the patient-by-patient comparison of all 27 patients who underwent surgery, the MR imaging diagnosis matched that of the histopathologic findings. There were no false-positive results of SPIO-enhanced MR studies.

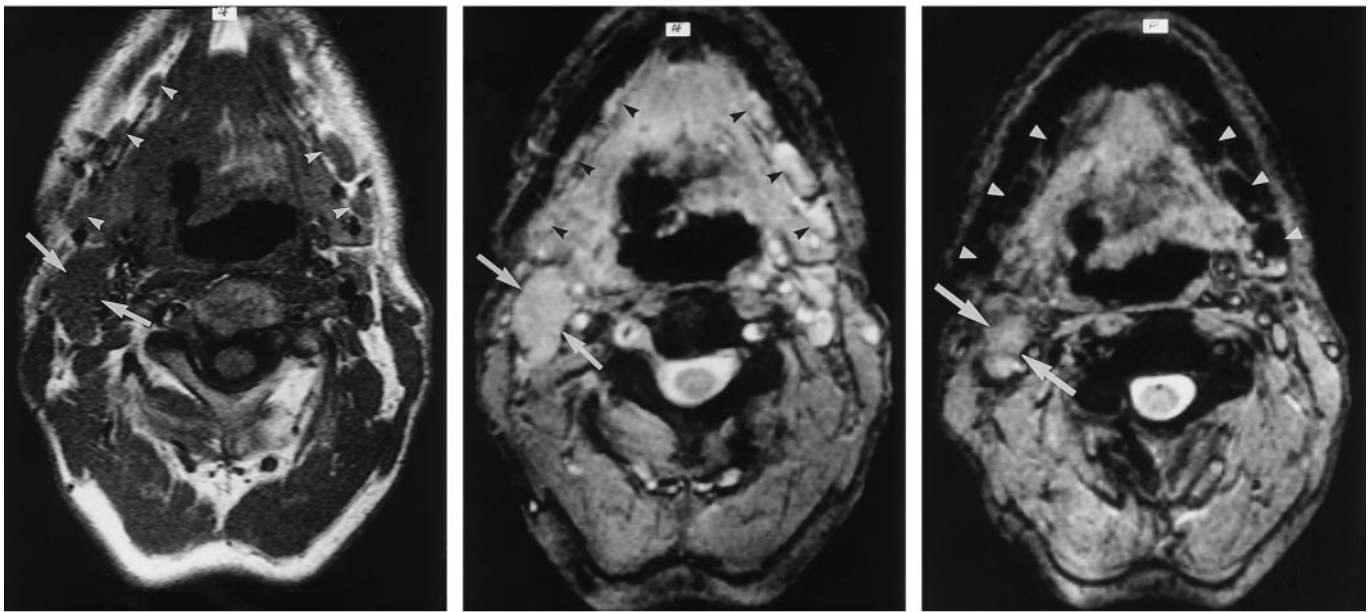


Figure 1. Tonsillar carcinoma and benign and malignant lymph nodes on both sides. (a) Transverse nonenhanced T1-weighted SE image (500/15) with lymph nodes in level I (arrowheads) on both sides and in level II (arrows) on the right side. (b) Transverse nonenhanced T2-weighted GRE image (500/15, 15° flip angle) demonstrates the lymph nodes in level I (arrowheads) on both sides and in level II (arrows) on the right side, with hyperintense signal. (c) Transverse SPIO-enhanced T2-weighted GRE image (500/15, 15° flip angle) obtained 30 hours after infusion of contrast material demonstrates no SI decrease in the lymph node in level II (arrows) on the right side, which represents lymph node metastasis. Note the SI decrease in the lymph nodes in level I (arrowheads) on both sides; this represents reactive lymph nodes.

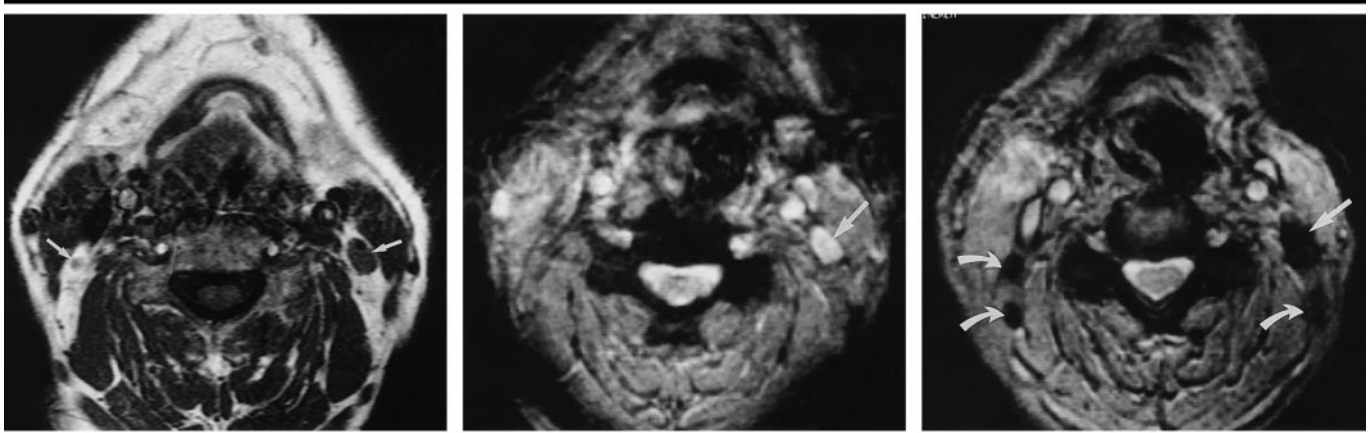


Figure 2. (a) Transverse nonenhanced T1-weighted SE image (500/15) shows a lymph node in level II on the left side (right arrow) and another lymph node in level II on the right side (left arrow). (b) Transverse nonenhanced T2-weighted GRE image (500/15, 15° flip angle) demonstrates the lymph node (arrow) in level II on the left side, with hyperintense signal pattern. The lymph node in level II on the right side is hard to delineate. (c) Transverse SPIO-enhanced T2-weighted GRE image (500/15, 15° flip angle) demonstrates SI decrease in the lymph node (straight arrow) in level II on the left side and a better visualization of the lymph nodes on both sides (curved arrows), which represents reactive lymph nodes.

Effect on Surgical Planning

In seven (26%) of 27 patients, findings of the MR studies influenced decisions relevant to therapy, including the surgical strategy. In five patients, MR imaging revealed additional lymph node metastases on the contralateral side, resulting in limited or radical neck dissection on the contralateral side. The contralateral lymph

node metastases were verified at histopathologic evaluation. In one patient with a primary tumor on the right side who was scheduled for radical neck dissection on that side, the side of radical neck dissection was changed because MR imaging enabled detection of a lymph node metastasis on the left side, which was verified with histopathologic evalua-

tion. Limited neck dissection performed on the right side in this patient revealed no lymph node metastases. MR imaging did not show any lymph node metastases on the right side, and this was verified at surgery. In one patient who was scheduled for radical neck dissection, no lymph node metastases were detected with MR imaging. Therefore, only a lim-

ited neck dissection was performed, and histopathologic evaluation also revealed no lymph node metastases in level II–IV. Also, a follow-up MR study 7 months later demonstrated no lymph node metastases or tumor recurrence.

DISCUSSION

The treatment of lymph node metastases of the head and neck region in patients with squamous cell carcinoma is a continuing source of controversy. The accuracy of imaging techniques, such as US, MR imaging, and CT, depends on the appropriateness of radiologic criteria used for diagnosing lymph node metastases. Size of nodes and evidence of necrosis are still the most important radiologic criteria. However, size as a criterion shows great variability; 6–30 mm is commonly used (3,10,11,13–20). Furthermore, studies have shown that the size criterion may differ depending on the level of the neck being examined (14). The size criterion is particularly important in the neck with no lymph node metastasis (N0). van den Brekel and co-workers (14) have clearly demonstrated that the commonly used criterion of approximately 10 mm (minimum transverse diameter) is not reliable and that the size criterion should be reduced for necks in which no lymph node metastases were detected during clinical examination. The optimal size criterion should be both highly sensitive and specific. A patient with squamous cell carcinoma of the head and neck and uncertain lymph node metastases obtains no benefit from a preoperative imaging method that is either highly specific or highly sensitive. van den Brekel and co-workers (14) have shown that a minimum transverse diameter of 7 mm for level II and 6 mm for the remainder of the neck revealed the optimal compromise between sensitivity and specificity in necks without palpable metastases. However, to our knowledge all previous studies attained a sensitivity of over 75% without sacrificing specificity. This is probably also caused by the prevalence of micrometastases, which in N0 necks is approximately 25% (21). SPIO-enhanced MR imaging of the neck provided a sensitivity of 86% and a specificity of 100% and is therefore one of the most promising modalities for the evaluation of the neck in patients with squamous cell carcinoma of the head and neck. Microinfiltration of lymph nodes will remain a problem even with high-spatial-resolution MR sequences.

A number of other studies were performed to analyze the value of techniques such as direct lymphangiography, interstitial lymphangiography with contrast agents such as SPIO (22–24) or gadolinium-diethylenetriamine pentaacetic acid-polyglucosylated macrocomplex (25), and intravenous lymphangiography (26,27) for the detection of lymph node metastases.

Furthermore, a variety of animal studies (28–30) and an initial patient study (26) have been performed to evaluate the potential of intravenous contrast material application for MR lymphography. Intravenous lymphography has several advantages compared with interstitial lymphangiography and direct lymphangiography. Intravenous administration provides homogeneous distribution throughout the body and is technically uncomplicated, less time-consuming, and virtually noninvasive.

In one study (31), two-dimensional proton MR spectroscopy helped differentiate primary squamous cell carcinoma and nodal metastases containing squamous cell carcinoma from normal tissue both in vitro and in vivo.

In clinical practice, a very sensitive test or criterion is needed to choose the proper treatment modality, because undertreatment is not as acceptable as overtreatment. Radical neck dissection is a highly invasive treatment that causes considerable cosmetic and functional problems. On the one hand, a radical neck dissection performed in a neck in which no metastasis has been detected would not be acceptable; a limited neck dissection would be adequate. On the other hand, leaving undetected lymph node metastases behind substantially worsens the prognosis. Furthermore, the decision for postoperative radiation therapy relies mainly on the node stage of the tumor. With regard to the therapeutic influence of imaging modalities in patients with lymph node metastases in the neck, the level-by-level evaluation is of critical importance. It is more important to rule out lymph node metastases in a given level than to determine the number within the level, because the entire level will have to be resected anyway.

SPIO-enhanced T2-weighted GRE sequences allowed easier detection of benign lymph nodes—particularly small nodes—because of the marked SI decrease after administration of contrast material. The best sequence for differentiating between benign and malignant lymph nodes was the SPIO-enhanced T2-weighted GRE two-dimensional sequence, because benign lymph nodes showed a

more obvious SI decrease. This sequence was superior to the SPIO-enhanced T2-weighted SE sequence. Neither the non-enhanced nor the SPIO-enhanced SE T1-weighted sequence was suited for differentiating between benign and malignant lymph nodes. SPIO-enhanced T1-weighted sequences could be eliminated in future use of this contrast material. SPIO-enhanced MR imaging had an important effect on surgical planning that was based on the detection of contralateral lymph node metastases that would have been undetected without SPIO enhancement. The contralateral lymph node metastases that would have been missed would result in an early recurrence. Micrometastases are still a problem mainly due to the limited resolution of MR imaging sequences. Newly available high-spatial-resolution T2-weighted sequences will further improve the detection of partial metastatic lymph node infiltrations.

One limitation of our study is that only lymph nodes from the resection side were evaluated and included in this study, thereby precluding a histopathologic correlation for all neck lymph nodes. Another limitation is that the reference standard (histopathologic evaluation of the specimen removed at surgery) could be affected by MR imaging, since the surgeons used the MR image for guidance. Nevertheless, our study shows that SPIO-enhanced MR imaging improves the preoperative evaluation of lymph node metastases in the neck. Of 1,029 evaluated lymph nodes, we were able to detect 59 of the 69 histopathologically proved lymph node metastases. By using SPIO-enhanced MR imaging, we were able to obtain the correct diagnosis in 96.3% in the level-by-level evaluation and in 100% in the side-by-side evaluation. The use of SPIO contrast material appears to improve the diagnostic value of MR imaging for the assessment of lymph nodes in patients with squamous cell carcinoma of the head and neck.

References

1. Sakai O, Curtin HD, Romo LV, Som PM. Lymph node pathology: benign proliferative lymphoma and metastatic disease. *Radiol Clin North Am* 2000; 38:979–998.
2. Bruneton JN, Roux P, Caramella E, Demard F, Vallicioni J, Chauvel P. Ear, nose, and throat cancer: ultrasound diagnosis of metastasis to cervical lymph nodes. *Radiology* 1984; 152:771–773.
3. Close LG, Merkel M, Vuitch MF, Reisch J, Schaefer SD. Computed tomographic evaluation of regional lymph node involvement in cancer of the oral cavity and oropharynx. *Head Neck* 1989; 11:309–317.

4. Feinmesser R, Freeman JL, Noyek AM, Birt BD. Metastatic neck disease: a clinical/radiographic/pathologic correlative study. *Arch Otolaryngol Head Neck Surg* 1987; 113:1307-1310.
5. Friedman M, Shelton VK, Mafee M, Bellity P, Grybauskas V, Skolnik E. Metastatic neck disease: evaluation by computed tomography. *Arch Otolaryngol* 1984; 110:443-447.
6. Mancuso AA, Maceri D, Rice D, Hanafee W. CT of cervical lymph node cancer. *AJR Am J Roentgenol* 1981; 136:381-385.
7. Som PM. Lymph nodes of the neck. *Radiology* 1987; 165:593-600.
8. Stevens MH, Harnsberger HR, Mancuso AA, Davis RK, Johnson LP, Parkin JL. Computed tomography of cervical lymph nodes: staging and management of head and neck cancer. *Arch Otolaryngol* 1985; 111:735-739.
9. Steinkamp HJ, Cornehl M, Hosten N, Pegios W, Vogl T, Felix R. Cervical lymphadenopathy: ratio of long- to short-axis diameter as a predictor of malignancy. *Br J Radiol* 1995; 68:266-270.
10. Steinkamp HJ, Hosten N, Richter C, Schedel H, Felix R. Enlarged cervical lymph nodes at helical CT. *Radiology* 1994; 191:795-798.
11. Friedman M, Roberts N, Kirshenbaum GL, Colombo J. Nodal size of metastatic squamous cell carcinoma of the neck. *Laryngoscope* 1993; 103:854-856.
12. Shah JP, Strong E, Spiro RH, Vikram B. Surgical grand rounds: neck dissection—current status and future possibilities. *Clin Bull* 1981; 11:25-33.
13. van den Brekel MW, Stel HV, Castelijns JA, et al. Cervical lymph node metastasis: assessment of radiologic criteria. *Radiology* 1990; 177:379-384.
14. van den Brekel MW, Castelijns JA, Snow GB. The size of lymph nodes in the neck on sonograms as a radiologic criterion for metastasis: how reliable is it? *AJNR Am J Neuroradiol* 1998; 19:695-700.
15. Bruneton JN, Balu-Maestro C, Marcy PY, Melia P, Mourou MY. Very high frequency (13 MHz) ultrasonographic examination of the normal neck: detection of normal lymph nodes and thyroid nodules. *J Ultrasound Med* 1994; 13:87-90.
16. Stern WBR, Silver CE, Zeifer BA, Persky MS, Heller KS. Computed tomography of the clinically negative neck. *Head Neck* 1990; 12:109-113.
17. Som PP. Detection of metastases in cervical lymph nodes: CT and MR criteria and differential diagnosis. *AJR Am J Roentgenol* 1992; 158:961-969.
18. Hillsamer PJ, Schuller DE, McGhee RB, Chakeres D, Young DC. Improving diagnostic accuracy of cervical metastases with computed tomography and magnetic resonance imaging. *Arch Otolaryngol Head Neck Surg* 1990; 116:1297-1301.
19. Mancuso AA, Harnsberger HR, Muraki AS, Stevens MH. Computed tomography of cervical and retropharyngeal lymph nodes: normal anatomy, variants of normal, and applications in staging head and neck cancer. II. Pathology. *Radiology* 1983; 148:715-723.
20. Vassallo P, Wernecke K, Roos N, Peters PE. Differentiation of benign from malignant superficial lymphadenopathy: the role of high resolution US. *Radiology* 1992; 183:215-220.
21. van den Brekel MW, van der Waal I, Meijer CJ, Freeman JL, Castelijns JA, Snow GB. The incidence of micrometastases in neck dissection specimens obtained from elective neck dissections. *Laryngoscope* 1996; 106:987-991.
22. Hamm B, Taupitz M, Hussmann P, Wagner S, Wolf KJ. MR lymphography with iron oxide particles: dose-response studies and pulse sequence optimization in rabbits. *AJR Am J Roentgenol* 1992; 158:183-190.
23. Taupitz M, Wagner S, Hamm B, Diene-mann D, Lawaczek R, Wolf KJ. MR lymphography using iron oxide particles: detection of lymph node metastases in the VX2 rabbit tumor model. *Acta Radiol* 1993; 34:10-15.
24. Weissleder R, Elizondo G, Josephson L, et al. Experimental lymph node metastases: enhanced detection with MR lymphography. *Radiology* 1989; 171:835-839.
25. Harika L, Weissleder R, Poss K, Zimmer C, Papisov MI, Brady TJ. MR lymphography with a lymphotropic T1-type MR contrast agent: Gd-DTPA-PGM. *Magn Reson Med* 1995; 33:88-92.
26. Anzai Y, Blackwell KE, Hirschowitz SL, et al. Initial clinical experience with dextran-coated superparamagnetic iron oxide for detection of lymph node metastases in patients with head and neck cancer. *Radiology* 1994; 192:709-715.
27. Anzai Y, McLachlan S, Morris M, Saxton R, Lufkin RB. Dextran-coated superparamagnetic iron oxide: an MR contrast agent for assessing lymph nodes in the head and neck. *AJNR Am J Neuroradiol* 1994; 15:87-94.
28. Guimaraes R, Clement O, Bittoun J, Carnot F, Fria G. MR lymphography with superparamagnetic iron nanoparticles in rats: pathologic basis for contrast enhancement. *AJR Am J Roentgenol* 1994; 162:201-207.
29. Harika L, Weissleder R, Poss K, Papisov MI. Macromolecular intravenous contrast agent for MR lymphography: characterization and efficacy studies. *Radiology* 1996; 198:365-370.
30. Elste V, Wagner S, Taupitz M, et al. Magnetic resonance lymphography in rats: effects of muscular activity and hyperthermia on the lymph node uptake of intravenously injected superparamagnetic iron oxide particles. *Acad Radiol* 1996; 3:660-666.
31. Mukherji SK, Schiro S, Castillo M, Kwock L, Muller KE, Blackstock W. Proton MR spectroscopy of squamous cell carcinoma of the extracranial head and neck: in vitro and in vivo studies. *AJNR Am J Neuroradiol* 1997; 18:1057-1072.